On the linear and non-linear electronic spectroscopy of chlorophylls: a computational study

Journal Name

Dynamic Article Links ►

Cite this: DOI: 10.1039/c0xx00000x

www.rsc.org/xxxxxx

ARTICLE TYPE

On the Linear and Non-linear Electronic Spectroscopy of Chlorophylls: A Computational Study

Alicja Graczyk, Justyna M. Żurek and Martin J. Paterson*

Institute of Chemical Sciences, Heriot Watt University, Edinburgh, EH14 4AS, United Kingdom

Received (in XXX, XXX) Xth XXXXXXXXX 20XX, Accepted Xth XXXXXXXXX 20XX
DOI: 10.1039/b000000x

A theoretical analysis of linear and non-linear (two-photon absorption) electronic spectroscopy of all known porphyrinic pigments has been performed using linear and quadratic density functional response theory, with long-range corrected CAM-B3LYP functional. We find that higher Soret transitions often contain non-Gouterman contributions and that each chlorophyll has the possibility for resonance enhanced TPA in the Soret region, although there are also significant TPA in the Q region.

Introduction

Spectroscopic properties of porphyrins and their structural analogues have captured significant attention of both experimental and theoretical chemists, and have been comprehensively studied since the middle of the twentieth century. The initial purpose of such research was to acquire knowledge of porphyrins' roles in fundamental biochemical processes including photosynthesis and respiration.[1] In more recent times it has been discovered that porphyrins and their derivatives can be successfully used in many modern technologies, for example, they can be employed as agents increasing the efficiency of solar cells,[2] charge generation materials for laser printers,[3] photosensitizers for use in photodynamic therapy[4] (PDT) and potential artificial blood components.[5] The effectiveness of processes involving the family of porphyrins is often related to both linear and non-linear optical properties of these molecules. This paper will focus on studies of linear and non-linear optical properties of known types of chlorophylls. Most chlorophylls are based on a reduced porphyrin macrocycle called chlorin.[1, 6, 7] Currently five types of chlorophylls are known: chlorophyll *a*, *b*, *c*, *d* and *f*, which display small structural differences from each other. Chlorophyll *c* exists in three forms (*c1*, *c2* and *c3*) and it is the only known chlorophyll, which is porphyrin rather than chlorin based (Fig. 1).[8-10]

Chlorophylls participate in the most fundamental reaction for living organisms, photosynthesis.[1, 11]. Through the production of carbohydrates and molecular oxygen, photosynthesis, directly or indirectly, supports most life on our planet. Chlorophylls form part of the photosynthetic apparatus and contribute to its stabilisation. They are collected in chloroplasts in plants, which are one of the building blocks of the photosynthetic antenna.[12] They participate in the first stage of photosynthesis, so-called light reactions. Their role can be briefly described as capturing photons of light and transferring the excitation energy to nearby reaction centres in the process of Förster resonance energy transfer.[13]

(a)

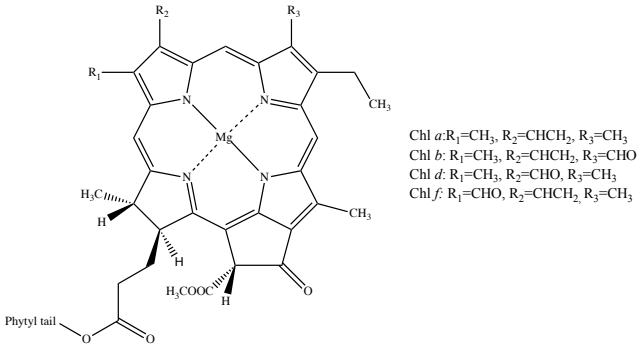

(b)

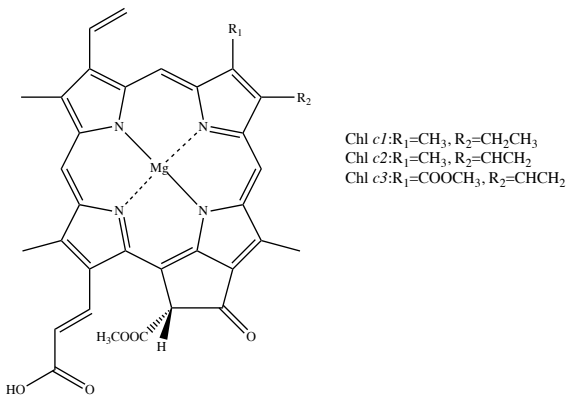

Fig. 1 Structures of chlorophylls (a) a, b, d and f (b) c1, c2, c3

The most abundant type of photosynthetic pigment is chlorophyll

a, which was the first one isolated (in 1817) and has been the most frequently studied. Chlorophyll *f*, on the other hand, is a very recent discovery. It was first recognized and described in the second half of 2010.[14] As a consequence, very little research has been done on this molecule.

The family of chlorophyll molecules covers most of the photosynthethically useful spectrum with extremely intense absorptions in the blue – the Soret band (330-480 nm), also called the B band and less intense red regions – Q bands (620-1050 nm).[7] Such a long absorption range makes chlorophylls good systems for OPA and TPA studies with potential applications in ecophysiology, biochemistry, biophysics and also medicine. TPA studies have seen especially increasing importance in recent years. This is due to their wide applications in fluorescence imaging, photonics, optical data storage, and most importantly production of singlet oxygen with applications in photodynamic anticancer therapy.[15-20] Anticancer photodynamic therapy is a relatively new branch of medical technology, which requires a photosensitizer, light of a wavelength suitable for the absorption by the photosensitizer, and molecular oxygen.[21] The absorption properties of a photosensitizer are clearly very important. A PDT drug must be able to absorb in the therapeutic window, which ranges from 600 and 800 nm. Light absorption and scattering in tissue depend on the wavelength of the electromagnetic radiation. The optical window for tissue penetration lies in the range of 600-1300 nm. Its lower limit is set by principal tissue chromophores, such as melanin, haemoglobin and cytochromes, which have high absorption bands below 600 nm. The upper limit is set by the water absorption of near infrared light.[22] The other important aspect is that light of a wavelength exceeding 800 nm is unable to activate the photosensitizer. Therefore the search for ideal photosensitizers concentrates on ones absorbing in the red, which posses a high tissue penetration power and are energetic enough to produce singlet oxygen. In a TPA process the electronic transition of a molecule can be thought of as the simultaneous absorption two photons. The use of this non-linear technique in PDT has been an attractive alternative to OPA since the development of high-power femtosecond lasers.[23] One of the advantages of TPA over OPA includes the fact that the population of the excited state is quadratically proportional to the incident light intensity, therefore the maximum absorption occurs at the focal point of the laser beam.[24] Because of this, there is potential to provide highly targeted treatment for tumours, since excitation can be pin-pointed to small volumes at the focus of a laser.[17] Another advantage of TPA is the possibility to use pulses of light in the near-infrared region (750-900 nm). Because light with this wavelength penetrates tissue more deeply than visible light, PDT therapy can be more effective. Also TPA opens the possibility of excitations forbidden in OPA.[25] Nonlinear spectroscopy is however very challenging to study both experimentally or theoretically. There have been a few experimental studies on TPA spectroscopy of chlorophylls and other organic pigments[26-30] but very little on their computational modelling.[31, 32] There is however much more computational research on OPA spectroscopy of chlorophylls.[33-42] In 1960 the American theoretical chemist Gouterman developed a theory of metal-free porphyrin UV-Vis spectra, the so-called four-orbital model, which describes positions and character of main electronic transitions in such systems.[1, 43] Later this theory was extended to porphyrins containing metal ions. According to this model, the Soret and the Q bands are the result of the electronic transitions between four orbitals, i.e., HOMO and HOMO-1 π orbitals to LUMO and LUMO+1 π^* orbitals. These orbitals are centered on the porphyrin core. In a metal-containing D_{4h} porphyrin, the LUMO and LUMO+1 π^* orbitals are degenerate by symmetry, while the HOMO and HOMO-1 π orbitals are nearly degenerate. Gouterman labeled the HOMO orbitals as a_{1u} and a_{2u}, while LUMO orbitals were designated e_{gy} and e_{gx}. Therefore the possible transitions between these orbitals are $a_{1u} \rightarrow e_{gy}$ and $a_{2u} \rightarrow e_{gx}$, having *x* polarization, and $a_{1u} \rightarrow e_{gx}$ and $a_{2u} \rightarrow e_{gx}$, having *y* polarization. *X* and *y* polarized excited states are further mixed and split in energy by configuration interaction and form two transitions of low intensity and energy transitions (Q_x and Q_y, with Q_y being a lower energy transition than Q_x and also higher intensity), and two high intensity and higher energy transitions (B_x and B_y).[1] Some recent studies of OPA of chlorophylls and similar systems will now be presented. Linnanto et al performed studies on spectroscopic properties of *a*, *b*, *c1*, *c2*, *c3*, *d* chlorophylls using semi-empirical ZINDO/S CIS (15,15) and PM3 CISD (5,5) methods and also ab-initio CIS (5,5)/6-31G(d) method.[37] Ab-initio CIS(5,5) methods turned out to overestimate the transition energies of the lowest excited states of studied chlorophylls while the obtained energies when using semi-empirical methods were very close to experiment. This is not a surprise as semi-empirical methods use experimental parametrisation. The semi-empirical PM3 CISD (5,5) method had problems with predicting oscillator strengths of studied transitions. Vokáčová and Burda used TD-DFT to study the spectroscopy of chlorophyll *a*, *b*, *c1*, *c2*, *c3*, *d*, different bacteriochlorophylls, phycobilins and carotenoids.[35] In the case of (bacterio)-chlorophylls the phytyl chain was removed from the structure and replaced by a methyl group. TD-DFT with the B3PW91 functional and 6-31+G(d) basis set were used. The authors have obtained qualitatively good agreement with experimental spectra. The calculated values for the Q_y band were blueshifted in comparison to experiment by about 60-80 nm and about 20-30 nm for the Q_x and Soret (B) bands. The four orbital model of Gauterman turned out to be a reasonably good approximation within TD-DFT. The main electronic transitions were based mainly on four Gouterman MOs. Other studies by the Amos group include TD-DFT, CASPT2 and SAC-CI (symmetry-adapted cluster-configuration interaction) calculations on chlorophyll *a*, porphyrin and two oligoporphyrins of charge transfer N-band transitions located between Q and Soret bands.[38] For TD-DFT studies different functionals with a 6-31G(d) basis set were used. Due to the poor description of charge transfer processes by standard DFT functionals the authors used long-range corrected TD-CAM-B3LYP and compared the results against the current-density functional (CDFT) of van Faassen, de Boeij, van Leeuwen, Berger, and Snijders which was found to provide a good description of long-range interactions of some conjugated systems. SAOP GGA, B3LYP and BP86 functionals were also used for completeness. They have found that amongst all DFT methods used only CAM-B3LYP properly predicts HOMO-LUMO energy gaps and also positions and character of

charge transfer bands between Q and Soret bands in chlorophyll *a* and other systems. In general CASPT2 results with a (16,15) active space were the most qualitatively accurate and the reason for it could be a contribution from double or higher excitations. However, this is also the most expensive method, which requires a lot of computational and chemical insight. SAC-CI and CAM-B3LYP results were found to overestimate the Q-Soret splitting but overall were also in reasonable agreement with experimental values. Due to the large computational scaling of SAC-CI method it was concluded that CAM-B3LYP amongst all is the easiest and at the same time cost-effective method, which gives applicable accuracy for systems where charge-transfer states may be of importance.

Due to the important chlorophyll applications mentioned above understanding the interaction of light with chlorophylls is crucial. This paper will focus on studies of the OPA and also TPA spectra of all up to date known chlorophylls *a-f* using time-dependent response density functional theory with the CAM-B3LYP functional which was previously found to give very reliable results for OPA and TPA studies, on a wide range of systems, due to its correct asymptotic behaviour.[31, 44-46] Such full linear and nonlinear spectroscopic studies on all known chlorophylls have not been performed to date.

Methods

Theory and Computational Details

Linear and quadratic density functional response theory (commonly known as Time-Dependent Density Functional Theory, TD-DFT)[47] has been used to study linear and nonlinear spectroscopy of chlorophylls. TD-DFT uses the stationary density and instantaneously switches on a time dependent field as a perturbation, then determines the response of the density to the perturbation. Excitation energies are given by the poles of the linear response function, while OPA and TPA transition strengths are obtained as residues of the linear and quadratic response functions respectively. To determine the transition strength of a given state for a TPA, the first residue of quadratic response function needs to be considered. This gives the two-photon transition tensor T (which can be written in a sum over states (SOS) formalism):

$$T_{\alpha\beta} = \sum_j \frac{\langle 0|\mu_\alpha|j\rangle\langle j|\mu_\beta|f\rangle}{\omega_j - \omega} + \frac{\langle 0|\mu_\alpha|j\rangle\langle j|\mu_\beta|f\rangle}{\omega_j - \omega}$$

0 represents the ground state, *j* an intermediate state and *f* the final state, while ω_j shows the excitation frequency of the *j*th state, ω the frequency of the irradiating light, μ_α and μ_β denoting the spatially dependent components of the electric dipole operator (with α and β indicating the Cartesian coordinates *x*, *y* and *z*). Thus, the virtual state in TPA is written as a sum over all intermediate (real eigenstates) of the system. This SOS expression is not calculated explicitly in response theory, as it calculates the TPA transition directly without constructing each state.[48] Nevertheless the SOS expression is very useful for analysis. Using T one can then calculate the two-photon absorption transition strength δ, which is determined by,

$$\delta^{TP} = F\delta_F + G\delta_G + H\delta_H$$

$$\delta_F = \frac{1}{30}\sum_{Y,Z} T_{YY}T^*_{ZZ}$$

$$\delta_G = \frac{1}{30}\sum_{Y,Z} T_{YZ}T^*_{YZ}$$

$$\delta_H = \frac{1}{30}\sum_{Y,Z} T_{YZ}T^*_{ZY}$$

The coefficients F, G and H are based on the polarisation of the incident photons and in this paper they will be used for conditions of parallel linearly polarised light beams, thus F=G=H=2. Experimentally the two-photon absorption cross sections of molecules are reported in Goeppert-Mayer (GM) units, where 1 GM equals 10^{-50} cm^4s $photon^{-1}$ $molecule^{-1}$. However, in this work the TPA cross-sections (here directly transition strengths) are shown in atomic units.[48]

The structure of chlorophyll *a* found in Chemical Entities of Biological Interest (ChEBI) database was chosen for initial studies.[49] The influence of phytyl tail on spectroscopic properties of chlorophyll *a* was examined and found to be minimal and so for further studies it was replaced with methyl group to reduce the computational cost. This is presented in Figure S1 of supporting information. Other conformers of chlorophyll *a* with methyl instead of phytyl tail were built based on ChEBI structure and their total free energies compared. Similarly conformers of other chlorophylls were built by changing appropriate ligands as shown in Fig. 1. The effect of basis set on the (geometrical) structure of a simple chlorophyll model was examined using 6-31G(d), cc-pVDZ, cc-pVTZ, aug-cc-pVDZ basis sets, and on the spectral properties using 6-31G(d), cc-pVDZ, cc-pVTZ basis sets, and it was found to be of minor importance. Thus for our studies 6-31G(d) basis set was used as a cost effective choice. The influence of different DFT functionals on the structure of the same chlorophyll model gave only minimal changes in bond lengths (~0.01-0.02Å) and angles (<1°). The geometries of all studied chlorophylls *a-f* and their conformers were optimised using the CAM-B3LYP functional and 6-31G(d) basis set. The structures of each chlorophyll having the lowest total free energy were chosen for further spectroscopic studies. The effect of DFT functional on the spectroscopic features of chlorophyll *a* was examined using B3PW91, B3LYP, CAM-B3LYP, and BP86. These results are presented in SI Figure S2 and S3. The qualitative spectral features of chlorophyll *a* calculated with these functionals are very similar. The positions of the Q bands with B3PW91, B3LYP and CAM-B3LYP were almost the identical, and only differed slightly in intensity. An approximately 20 nm red-shift was observed for BP86 comparing to other functionals. The positions of the B bands slightly differ between different functionals used, with the CAM-B3LYP obtained B band being the most blue-shifted compared to experiment and BP86 the least. As mentioned in the introduction the CAM-B3LYP functional is known to properly describe the HOMO-LUMO energy gaps, positions and character of charge transfer bands between Q and B bands in such systems thus TD-CAM-B3LYP with the 6-31G(d) basis set was used for further study of OPA spectra. In the computed spectra two different phenomenological broadening factors were considered. A 20 nm Gaussian broadening factor

was chosen to compare the computed spectra with the experimental ones. The stick spectrum, produced by applying the broadening factor 0.5 nm was generated in order to illustrate the electronic transitions. The effect of solvent on spectra was examined using the SMD model[50] with diethyl ether as a solvent for chlorophylls *a-d* and methanol for chlorophyll *f* for better comparison of calculated UV-Vis spectra with experiment. The first 15 excited states were considered for both OPA and TPA spectroscopic properties of all studied chlorophylls. The Gaussian 09c program was used for all geometry optimisations and OPA calculations, whereas TPA CAM-B3LYP studies were performed using the Dalton 2011 program.

Results and discussion

One-photon Absorption (OPA)

Experimental and theoretical bands in the gas phase have been plotted against each other in order to determine systematic shifts for these types of systems. A reasonably systematic correlation between theory and experiment of the spectral features is achieved here, this is presented in Figure S4 of supporting information. All theoretical spectra are systematically blue-shifted compared to the experimental ones. Table 1 presents the main calculated OPA transitions in the gas phase and in the solution as well as spectral bands determined experimentally. Figures S5-S7 in supporting information present a visual comparison of theoretical and experimental spectra for chlorophylls *a*, *b* and *f*. The calculated spectra of all studied chlorophylls compare qualitatively with experimental studies. Three main spectroscopic bands Q_y, Q_x and B have been localised. The intensity of the calculated Soret band B, as experimentally expected, is much larger then the intensity of Q bands; also Q_y band is more intense then Q_x band. Generated pictures of the OPA spectra in the gas phase and the character of main transitions involved in these bands are also presented in Table 1. More detailed analysis of single-particle hole transitions is presented in Figure S8-S14 of supporting information. As mentioned above it is evident is that all peaks in the computed spectra are blue-shifted in comparison with the experimental spectrum. There is a blue shift of around 90 nm to a 110 nm for Q_y bands of chlorophylls *a*, *b* and *f*. The smallest blue shift here for Q_y band of around 90 nm is observed for chlorophyll *a* and the biggest for chlorophyll *f*, 110 nm. For Q_x bands of these systems, the smallest blue shift is observed for chlorophyll *a* (around 80nm) and the largest blue shift is observed for chlorophyll *f* (around 140nm). Chlorophylls *c1*, *c2*, *c3* and *d* show around a 60-70 nm blue shift for Q_y bands, 25-40 nm blue shift for Q_x bands which is in better comparison with experimental studies. All the chlorophylls studied show a blue shift of around 70-80 nm for the Soret - B bands. Since it has been reported that the presence of the solvent shifts porphyrin spectra to the red region,[51] the difference in the position of the computed and experimental peaks could be attributed to this phenomenon. Looking at the spectral bands calculated using the SMD solvent model[50] with appropriate solvent it could be noticed that indeed it is the case. Including a solvent in the calculation moves the position of the peaks to the red region of around 5-20 nm for Q and B bands of all chlorophylls.

Table 1. Experimental and computed one-photon absorption (OPA) transitions of chlorophylls *a-f*. TD-CAMB3LYP with 6-31G(d) basis set used for computational studies.

Method	TD-CAM-B3LYP (Gas phase)[a]	TD-CAM-B3LYP (SMD model)	Experiment[b]
Chlorophyll *a* 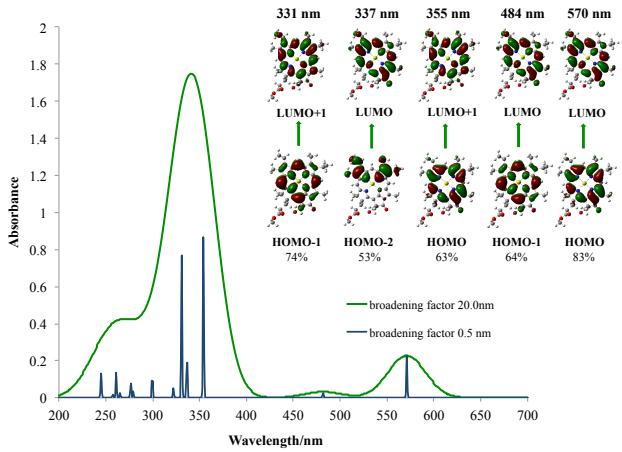			
λ [nm] Qy Osc. str. λ [nm] Qx Osc. str. λ [nm] B Osc. str.	570 0.2281 484 0.0273 355 0.9272 337 0.2517 331 0.8331	581 0.3243 488 0.0602 370 1.1871 345 0.7728 341 0.4852	662 - 578 - 430 -
Chlorophyll *b* 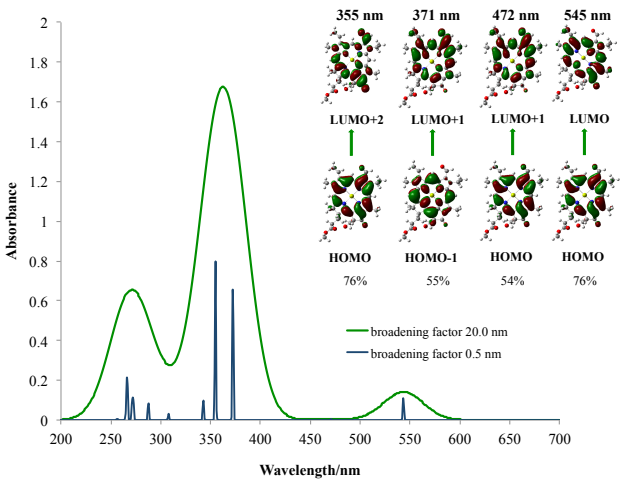			
λ [nm] Qy Osc. str. λ [nm] Qx Osc. str. λ [nm] B Osc. str.	545 0.1456 472 0.0062 371 0.9995 355 0.8721	552 0.2045 475 0.0127 390 1.3133 369 0.9854	644 - 549 - 455 -
Chlorophyll *c1*			

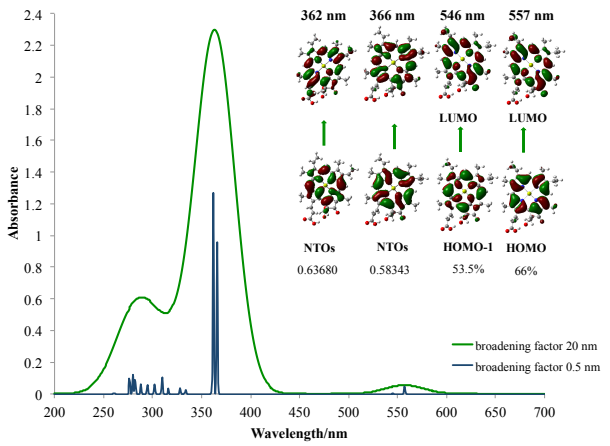

λ [nm] Qy	557	562	628
Osc. str.	0.0538	0.0827	-
λ [nm] Qx	546	549	578
Osc. str.	0.0011	0.0024	-
λ [nm] B	366	384	444
Osc. str.	1.0082	1.4998	-
	362	381	
	1.2758	1.3679	

Chlorophyll *c2*

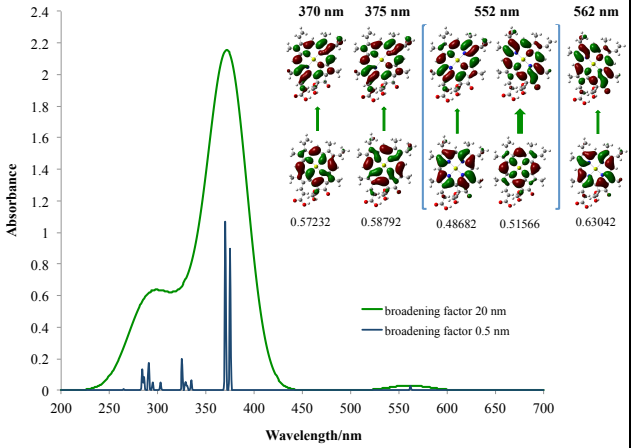

λ [nm] Qy	562	566	628
Osc. str.	0.0284	0.0421	-
λ [nm] Qx	552	556	579
Osc. str.	0.0029	0.0016	-
λ [nm] B	375	392	448
Osc. str.	0.9328	1.366	-
	370	390	
	1.1987	1.411	

Chlorophyll *c3*

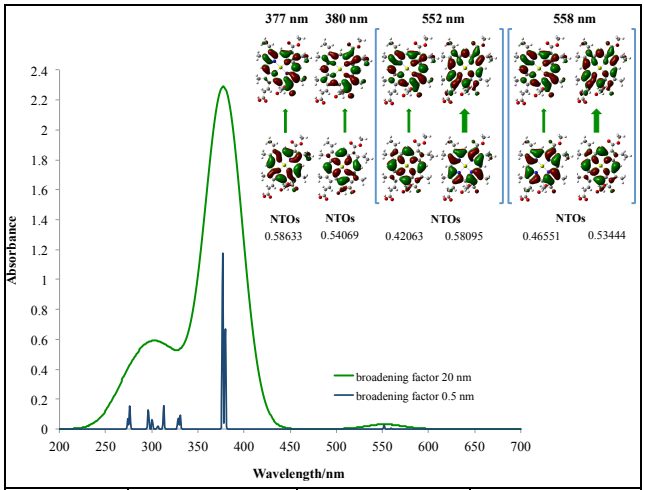

λ [nm] Qy	559	562	626
Osc. str.	0.0035	0.0019	-
λ [nm] Qx	552	555	586
Osc. str.	0.0279	0.0402	-
λ [nm] B	380	397	452
Osc. str.	0.9088	1.4682	-
	377	396	
	1.3752	1.3897	

Chlorophyll *d*

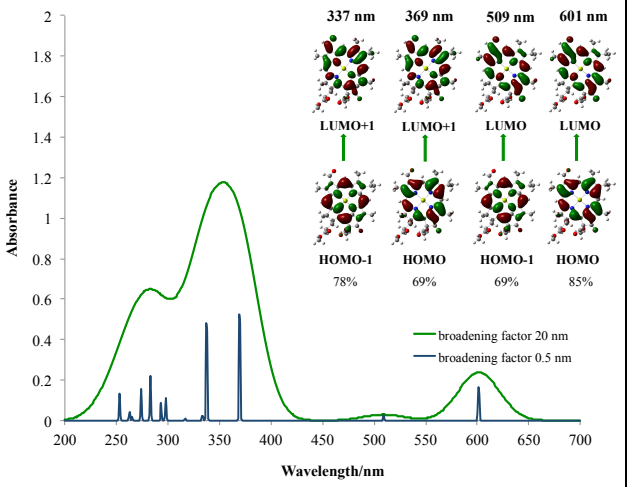

λ [nm] Qy	601	616	668
Osc. Str.	0.2383	0.3302	-
λ [nm] Qx	509	516	-
Osc. str.	0.0296	0.058	-
λ [nm] B	369	386	447
Osc. str.	0.8243	1.0409	-
	342	349	
	0.0004	0.9564	
	337		
	0.7563		

Chlorophyll *f*

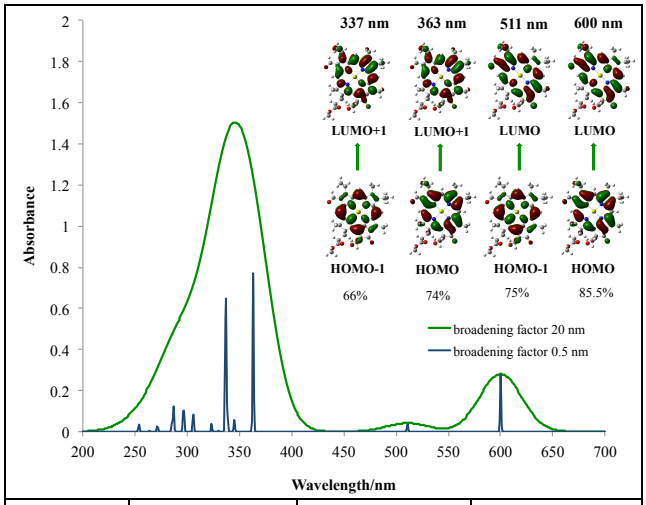

λ [nm] Qy	600	620	712
Osc. str.	0.2801	0.4228	-
λ [nm] Qx	511	518	654
Osc. str.	0.0413	0.0965	-
λ [nm] B	363	375	444
Osc. str.	0.7866	0.9062	-
	345	346	408
	0.0579	1.1823	-
	338		
	0.1443		
	337		
	0.7992		

[a] TD-CAM-B3LYP computed spectra in the gas phase with two different Gaussian broadening factors of 20 and 0.5 nm, the character of main transitions, and their contribution in % for canonical orbitals or 1-particle transition density matrix eigenvalues for natural transition orbitals (NTOs).

[b] Experimental bands for chlorophylls *a-d* recorded in diethyl ether solvent[7] and chlorophyll *f* in methanol[14]

The average red shift for Q_x bands here of around 5 nm is observed for chlorophylls *a-c3* and *f*. The smallest influence of the solvent on the Q_y bands is observed for chlorophyll *c3* (3nm) and the largest for chlorophyll *f* (20nm). The chemical nature of main spectroscopic bands have been shown in the right part of each spectrum and is determined by studying the canonical Kohn-Sham orbitals that take part in main electronic transitions present. From this it can be seen that the two main transitions in the Soret band as well as transitions in the Q_y and Q_x bands are all between the frontier molecular orbitals located on chlorophyll core, as predicted by Gouterman. Due to some orbital mixing present for chlorophylls *c1*, *c2* and *c3* Natural Transition Orbitals (NTOs)[52] were used to determine their main excitations, which in the end also resembled Gouterman orbitals. For Soret band of chlorophyll *a* it has been noticed that HOMO-2 orbital becomes significant and for chlorophyll *b*, LUMO+2 orbital. This has been already seen for spectroscopy of porphycene core based systems and may imply that the Gouterman model should be treated in caution when discussing Soret bands of these systems.[45, 53] No charge transfer transitions have been observed. In Table 1 only the largest contributions to transitions have been shown. A detailed analysis of the spectral character of studied chlorophylls is presented in supporting information Figures S8-S14. From these results it can be concluded that calculated spectra are qualitatively very well comparable with experimental ones and can be used to help rationalise and assign experimental spectra of porphyrins and derivatives based on general trends, although quantitative spectral data is still problematic with TD-DFT.

Two-photon Absorption (TPA)

TPA calculations were conducted for the first fifteen excited states of each chlorophyll using the CAM-B3LYP functional with a 6-31G(d) basis set in the gas phase. It has been shown before that this method gives reliable results for TPA spectroscopic properties of porphyrin systems comparing with experimental studies.[44] TPA computed results for chlorophylls *a*, *b*, *d* and and *f* are presented in Table 2 and for chlorophylls *c1*, *c2* and *c3* in Table 3. Since in TPA both photons are absorbed simultaneously (in this case two equal energy photons, i.e., resonant absorption), the photon wavelength is twice the wavelength presented (i.e., at the eigenstate energy). Some of the large numbers of TPA transition strengths for some excitations in chlorophyll molecules can be explained by the so-called *resonance enhancement* effect.[44, 54] The intensity of the absorption depends on the position of the virtual state (i.e., at half the excitation energy for two equal photons being absorbed). The phenomenon can be explained using the sum-over-states expression mentioned in theory section. Thus, the virtual state is written as a linear combination of all real eigenstates of the molecule. If the frequency of light is close to the frequency between the initial state and a real eigenstate then the denominator will cause the transition moment to tend to infinity. Therefore, the species with potentially very large δ will have the TPA absorption maxima equal or very close to half of the wavelength of Q_y in OPA.

Problems of standard molecular response theory can occur near the resonance region Soret because the excited states have infinite lifetimes when standard molecular functions are derived.[55] Thus, there have been damped response theory methods being developed to sort this problem, which removes the singularities of the response functions at the resonance frequencies.[55, 56] Even without using damped response theory standard method inform that there will be very large TPA cross sections in certain chlorophylls due to accidental degeneracy between Soret and Q states (table 4). Thus for example each chlorophyll has states in the Soret region with very large TPA cross sections but these are shifted relative to each other by the specific nature of the chlorophyll. This is similar to what is observed with electronic fine tuning of macrocyclic cores.[46] Also of interest here are the significant TPA in the Q region itself; although orders of magnitude less than resonance enhanced Soret TPA, it is still intense enough to be of interest in PDT as discussed above.

Table 2. CAM-B3LYP/6-31G(d) Calculated two-photon absorption (TPA) transitions λ [nm] and their TPA cross-sections δ [a.u.] for chlorophylls *a*, *b*, *d* and *f*.

Chlorophyll a		Chlorophyll b	
λ [nm]	δ [a.u.]	λ [nm]	δ [a.u.]
571	519	544	760
484	3220	473	3560
334	9080	371	4230
337	5850	355	460
332	676	341	2020
327	14.1	330	1.99
322	1460	323	3.04
299	58000	308	1160
279	74200	287	19600
275	2410000	272	3.62E+11
262	83500	271	71600000
259	241000	266	2580000
247	13600	263	306000
246	188000	257	7780
240	303000	257	8620
Chlorophyll d		Chlorophyll f	
λ [nm]	δ [a.u.]	λ [nm]	δ [a.u.]
602	473	599	478
508	3170	510	2820
369	18100	364	24200
342	1.78	345	2120
338	1500	339	295
334	49.9	337	3040
333	4030	330	12300
316	39600	323	10300
298	179000000	305	13800000
293	9500	297	300000000
283	1050000	287	1480000
274	65700	286	18600
263	148000	271	18400
253	2280000	254	31000000
251	576000	252	1750000

Table 3. CAM-B3LYP/6-31G(d) calculated two-photon absorption (TPA) transitions λ [nm] and their TPA cross-sections δ [a.u.] for chlorophylls *c1*, *c2*, and *c3*.

Chlorophyll *c1*		Chlorophyll *c2*		Chlorophyll *c3*	
λ [nm]	δ [a.u.]	λ [nm]	δ [a.u.]	λ [nm]	δ [a.u.]
558	191	561	202	558	47.2
546	148	554	256	551	457
366	230	376	305	379	282
363	439	370	269	377	243
333	828	335	325	337	1890
329	93.8	331	185	331	536
316	247	329	188	329	338
310	2050	325	1810	313	2440
302	951	309	3770	307	44800
294	59200	303	6480	300	2950
288	64200	295	59000	297	4320
282	28300	290	8680	296	4790
280	7460000	286	34200	280	571000
277	4280000	284	259000	276	6.5E+12
253	9030	263	4770	274	914000

Table 4. Positions of resonance enhancement peaks: the maximum absorption wavelengths for TPA (in the Soret region) and OPA (in the Q region).

System	Q region in OPA [nm]	Soret region in TPA [nm]
Chlorophyll *a*	570	275
Chlorophyll *b*	545	272
Chlorophyll *c1*	557	280
Chlorophyll *c2*	562	284
Chlorophyll *c3*	559	276
Chlorophyll *d*	601 509	298 253
Chlorophyll *f*	600 511	297 254

Conclusions

Theoretical OPA and TPA spectra of chlorophylls were calculated with TD-CAM-B3LYP functional with the 6-31G(d) basis set. It has been shown that this method to a good approximation describes the structural and spectroscopic properties of chlorophylls at a reasonable computational cost. Calculated OPA spectra were in good qualitative agreement with their experimental equivalents and the electronic transitions were studied in a more in-depth manner by examining the nature of the orbitals involved in the transitions. The position of linear electronic transition bands are blue-shifted in comparison to experiment but their relative intensities and chemical nature modelled quite well experimental findings. In general the Gouterman four-orbital model, which is frequently used to determine the character of main electronic transitions in porphyrins and similar systems turned out to be a good approximation for the red-region of the chlorophyll spectra. However, it has been found that for the Soret bands of some chlorophylls it is missing some crucial electronic contributions from higher lying orbitals, thus, it needs to be treated with caution when used for such systems. Using a solvent model, specifically the SMD model, in the calculations of the OPA spectroscopic properties had only a small red-shift effect. A more advanced model could be used, treating the solvent with discrete molecules in the first solvation sphere, using for example a QM/MM approach, which can be a perspective for future studies. It would be interesting to see if a better solvent model caused a larger red-shift closer to absolute experimental values. The maximum TPA absorption values of calculated chlorophylls are between 550-600 nm, showing large transition strengths, all studied chlorophylls could be potential candidates for use in photodynamic therapy. Also of interest here would be comparing Q band TPA with resonance enhanced Soret TPA. Engineering of new systems based on chlorophyll *d* and *f*, which look especially promising because their spectra are the most red-shifted amongst all chlorophylls, may be important for future TPA studies in the context of phototherapy. Other important areas of further research could include the spectroscopy of chlorophyll dimers, and larger aggregates and examination of how their spectra differ from those of single molecules. That research would be especially beneficial for PDT, as the concentration of photosensitizer often has to be quite high to use this form of treatment effectively.

Acknowledgements

We thank the European Research Council (ERC) for funding under the European Union's Seventh Framework Programme (FP7/2007-2013)/ERC Grant No. 258990, and the EPSRC for funding through grant EP/J006602.

Notes and references

*Corresponding author: m.j.paterson@hw.ac.uk

† Electronic Supplementary Information (ESI) available: The effect of phytyl tail presence on one-photon absorption spectra of chlorophyll *a;* TD-DFT functional comparison; comparison with experimental spectra; detailed transition analysis; Cartesian coordinates for all species studied. See DOI: 10.1039/b000000x/

1. Milgrom, L. R., *The colours of life : An introduction to the Chemistry of Porphyrins and Related Compounds*. Oxford University Press: Oxford ; New York, 1997; p VI.
2. Mozer, A. J.; Griffith, M. J.; Tsekouras, G.; Wagner, P.; Wallace, G. G.; Mori, S.; Sunahara, K.; Miyashita, M.; Earles, J. C.; Gordon, K. C.; Du, L. C.; Katoh, R.; Furube, A.; Officer, D. L., *J. Am. Chem. Soc.* **2009,** *131* (43), 15621.
3. Wöhrle, D.; Schnurpfeil, G.; Makarov, S. G.; Kazarin, A.; Suvorova, O. N., *Macroheterocycles* **2012,** *5* (3), 191.
4. Sternberg, E. D.; Dolphin, D.; Bruckner, C., *Tetrahedron* **1998,** *54* (17), 4151.
5. Twyman, L. J.; Ge, Y., *Chem. Commun.* **2006,** (15), 1658.
6. Kadish, K. M.; Smith, K. M.; Guilard, R., Chlorophylls and Bilins: Biosynthesis, Synthesis, and Degradation. In *The Porphyrin Handbook*, Academic Press: San Diego, 2000; Vol. 13.
7. Scheer, H., Chapter 3 Chlorophylls. In *Primary Processes of Photosynthesis, Part 1: Principles and Apparatus*, The Royal Society of Chemistry: 2008; Vol. 8, pp 101.
8. Dougherty, R. C.; Strain, H. H.; Svec, W. A.; Uphaus, R. A.; Katz, J. J., *J. Am. Chem. Soc.* **1966,** *88* (21), 5037.
9. Fookes, C. J. R.; Jeffrey, S. W., *J. Chem. Soc. Chem. Commun.* **1989,** (23), 1827.
10. Withers, N.; Haxo, F. T., *Plant Sci. Lett.* **1975,** *5* (1), 7.
11. Archer, M. D.; Barber, J., *Molecular to Global Photosynthesis*. Imperial College Press: River Edge, NJ, 2004.
12. Green, B. R.; Parson, W. W., *Light-harvesting antennas in photosynthesis*. Kluwer Academic: Dordrecht ; Boston, 2003; p xx.
13. Gunderson, V. L.; Wilson, T. M.; Wasielewski, M. R., *J. Phys. Chem. C* **2009,** *113* (27), 11936.
14. Chen, M.; Schliep, M.; Willows, R. D.; Cai, Z. L.; Neilan, B. A.; Scheer, H., *Science* **2010,** *329* (5997), 1318.
15. Parthenopoulos, D. A.; Rentzepis, P. M., *Science* **1989,** *245* (4920), 843.
16. Zheng, Q. D.; Xu, G. X.; Prasad, P. N., *Chem-Eur. J.* **2008,** *14* (19), 5812.
17. Ogawa, K.; Kobuke, Y., *Org. Biomol. Chem.* **2009,** *7* (11), 2241.
18. Zhao, P. D.; Chen, P.; Tang, G. Q.; Liu, J. W.; Lin, L.; Guo, P.; Yu, Q.; Yao, J.; Ma, D. M.; Zhang, G. L.; Chen, W., *Sci. China Ser. B* **2008,** *51* (6), 529.
19. He, G. S.; Tan, L.-S.; Zheng, Q.; Prasad, P. N., *Chem. Rev.* **2008,** *108* (4), 1245.
20. Copley, L.; van der Watt, P.; Wirtz, K. W.; Parker, M. I.; Leaner, V. D., *Int. J. Biochem. & Cell Biol.* **2008,** *40* (2), 227.
21. DeRosa, M. C.; Crutchley, R. J., *Coord. Chem. Rev.* **2002,** *233*, 351.
22. Fuchs, B.; Berlien, H.-P.; Philipp, C. M., The Laser's Position in Medicine. In *Applied Laser Medicine*, Berlien, H.-P.; Müller, G. J., Eds. Springer-Verlag Berlin: Heidelberg New York, 2003.
23. Meshulach, D.; Silberberg, Y., *Nature* **1998,** *396* (6708), 239.
24. Belfield, K. D.; Schafer, K. J.; Liu, Y. U.; Liu, J.; Ren, X. B.; Van Stryland, E. W., *J. Phys. Org. Chem.* **2000,** *13* (12), 837.
25. Atkins, P. W.; De Paula, J.; Friedman, R., *Quanta, Matter, and Change: A molecular approach to Physical Chemistry*. Oxford University Press: Oxford ; New York, 2009; p xxi.
26. Leupold, D.; Teuchner, K.; Ehlert, J.; Irrgang, K. D.; Renger, G.; Lokstein, H., *Biophys. J.* **2002,** *82* (3), 1580.
27. Zimmermann, J.; Linden, P. A.; Vaswani, H. M.; Hiller, R. G.; Fleming, G. R., *J. Phys. Chem. B* **2002,** *106* (36), 9418.
28. Linden, P. A.; Zimmermann, J.; Brixner, T.; Holt, N. E.; Vaswani, H. M.; Hiller, R. G.; Fleming, G. R., *J. Phys. Chem. B* **2004,** *108* (29), 10340.
29. Zeng, Y.; Wu, Y.; Li, D.; Zheng, W.; Wang, W. X.; Qu, J. N. Y., *Planta* **2012,** *236* (5), 1653.
30. Shima, S.; Ilagan, R. P.; Gillespie, N.; Sommer, B. J.; Hiller, R. G.; Sharples, F. P.; Frank, H. A.; Birge, R. R., *J. Phys. Chem. A* **2003,** *107* (40), 8052.
31. Vivas, M. G.; Silva, D. L.; de Boni, L.; Zalesny, R.; Bartkowiak, W.; Mendonca, C. R., *J. Appl. Phys.* **2011,** *109* (10).
32. Susumu, K.; Fisher, J. A. N.; Zheng, J. R.; Beratan, D. N.; Yodh, A. G.; Therien, M. J., *J. Phys. Chem. A* **2011,** *115* (22), 5525.
33. Konig, C.; Neugebauer, J., *Phys. Chem. Chem. Phys.* **2011,** *13* (22), 10475.
34. Sundholm, D., *Chem. Phys. Lett.* **1999,** *302* (5-6), 480.
35. Vokacova, Z.; Burda, J. V., *J. Phys. Chem. A* **2007,** *111* (26), 5864.
36. Shipman, L. L.; Cotton, T. M.; Norris, J. R.; Katz, J. J., *J. Am. Chem. Soc.* **1976,** *98* (25), 8222.
37. Linnanto, J.; Korppi-Tommola, J., *Phys. Chem. Chem. Phys.* **2000,** *2* (21), 4962.
38. Cai, Z. L.; Crossley, M. J.; Reimers, J. R.; Kobayashi, R.; Amos, R. D., *J. Phys. Chem. B* **2006,** *110* (31), 15624.
39. Alvarado-Gonzalez, M.; Flores-Holguin, N.; Glossman-Mitnik, D., *Int. J. Photoenergy* **2013**.
40. Li, Y.; Cai, Z.-L.; Chen, M., *J. Phys. Chem. B* **2013**.
41. Linnanto, J.; Korppi-Tommola, J., *J. Phys. Chem. A* **2001,** *105* (15), 3855.
42. Zucchelli, G.; Jennings, R. C.; Garlaschi, F. M.; Cinque, G.; Bassi, R.; Cremonesi, O., *Biophys. J.* **2002,** *82* (1), 378.
43. Gouterman, M., *J. Mol. Spec.* **1961,** *6*, 138.
44. Arnbjerg, J.; Jimenez-Banzo, A.; Paterson, M. J.; Nonell, S.; Borrell, J. I.; Christiansen, O.; Ogilby, P. R., *J. Am. Chem. Soc.* **2007,** *129* (16), 5188.
45. Bergendahl, L. T.; Paterson, M. J., *J. Phys. Chem. B* **2012,** *116* (39), 11818.
46. Bergendahl, L. T.; Paterson, M. J., *RSC Advances* **2013,** *3* (24), 9247.
47. Casida, M. E., *Recent Advances in Density Functional Methods, Part I.* World Scientific: Singapore, 1995.
48. Poulsen, T. D.; Frederiksen, P. K.; Jorgensen, M.; Mikkelsen, K. V.; Ogilby, P. R., *J. Phys. Chem. A* **2001,** *105* (51), 11488.
49. http://www.ebi.ac.uk/chebi
50. Marenich, A. V.; Cramer, C. J.; Truhlar, D. G., *J. Phys. Chem. B* **2009,** *113* (18), 6378.
51. Sankar, M.; Arunkumar, C.; Bhyrappa, P., *J. Porphyr. Phtalocya.* **2004,** *08* (12), 1343.
52. Martin, R. L., *J. Chem. Phys.* **2003,** *118* (11), 4775.
53. Hasegawa, J.-y.; Takata, K.; Miyahara, T.; Neya, S.; Frisch, M. J.; Nakatsuji, H., *J. Phys. Chem. A* **2005,** *109* (14), 3187.
54. Drobizhev, M.; Stepanenko, Y.; Dzenis, Y.; Karotki, A.; Rebane, A.; Taylor, P. N.; Anderson, H. L., *J. Am. Chem. Soc.* **2004,** *126* (47), 15352.
55. Kristensen, K.; Kauczor, J.; Kjaergaard, T.; Jorgensen, P., *J. Chem. Phys.* **2009,** *131* (4).
56. Norman, P., *Phys. Chem. Chem. Phys.* **2011,** *13* (46), 20519.

